Biosensors and Bioelectronics 155 (2020) 112111

Contents lists available at ScienceDirect

Biosensors and Bioelectronics

journal homepage: http://www.elsevier.com/locate/bios

Improving the reproducibility, accuracy, and stability of an electrochemical biosensor platform for point-of-care use

Lung-Chieh Chen [a,b,1], Erick Wang [a,1], Chun-San Tai [a,b,1], Yuan-Chen Chiu [a,b], Chang-Wei Li [a,c], Yan-Ren Lin [d,e,f], Tsung-Han Lee [a,d], Ching-Wen Huang [a,h,i], Jung-Chih Chen [a,g,**], Wen Liang Chen [a,*]

[a] Department of Biological Science and Technology, National Chiao Tung University, Hsinchu, Taiwan
[b] Institute of Molecular Medicine and Bioengineering, National Chiao Tung University, Hsinchu, Taiwan
[c] AllBio Life Inc, Taichung, Taiwan
[d] Department of Emergency Medicine, Changhua Christian Hospital, Changhua, Taiwan
[e] School of Medicine, Kaohsiung Medical University, Kaohsiung, Taiwan
[f] School of Medicine, Chung Shan Medical University, Taichung, Taiwan
[g] Institute of Biomedical Engineering, National Chiao Tung University, Hsinchu, Taiwan
[h] Department of Emergency, Shuang Ho Hospital, Taipei Medical University, New Taipei City, Taiwan
[i] Division of Thoracic Surgery, Department of Surgery, School of Medicine, College of Medicine, Taipei Medical University, Taipei, Taiwan

ARTICLE INFO

Keywords:
Semiconductor manufacturing technology
Biotin-streptavidin system
Label-free electrochemical platform
Point-of-care testing (POCT)

ABSTRACT

Electrochemical biosensors possess numerous desirable qualities for target detection, such as portability and ease of use, and are often considered for point-of-care (POC) development. Label-free affinity electrochemical biosensors constructed with semiconductor manufacturing technology (SMT)-produced electrodes and a streptavidin biomediator currently display the highest reproducibility, accuracy, and stability in modern biosensors. However, such biosensors still do not meet POC guidelines regarding these three characteristics. The purpose of this research was to resolve the limitations in reproducibility and accuracy caused by problems with production of the biosensors, with the aim of developing a platform capable of producing devices that exceed POC standards. SMT production settings were optimized and bioreceptor immobilization was improved through the use of a unique linker, producing a biosensor with exceptional reproducibility, impressive accuracy, and high stability. Importantly, the three characteristics of the sensors produced using the proposed platform all meet POC standards set by the Clinical and Laboratory Standards Institute (CLSI). This suggests possible approval of the biosensors for POC development. Furthermore, the detection range of the platform was demonstrated by constructing biosensors capable of detecting common POC targets, including circulating tumor cells (CTCs), DNA/RNA, and curcumin, and the devices were optimized for POC use. Overall, the platform developed in this study shows high potential for production of POC biosensors.

1. Introduction

Electrochemical biosensors possess a low sample volume requirement, a short detection time, high portability, and ease of use (Anik 2017; da Silva et al., 2017; Szunerits et al., 2019), and are often the foundation upon which various point-of-care (POC) products are developed. Currently, the most promising design for POC use is a label-free affinity electrochemical biosensor comprising semiconductor manufacturing technology (SMT)-produced electrodes and a biosynthesized streptavidin mediator. SMT enhances the consistency of electrode assembly to improve reproducibility (Hierlemann et al., 2003; Pohanka 2017). Label-free affinity detection offers ease of production and direct interaction with a wide range of targets, which expands the potential uses and improves the accuracy of the biosensors (Daniels and Pourmand 2007; Johnson and Krauss 2017). Streptavidin exhibits strong binding affinity for biotinylated bioreceptors and stabilizes bioreceptor

* Corresponding author. Department of Biological Science and Technology, National Chiao Tung University, Hsinchu, 30010, Taiwan, Republic of China.
** Corresponding author. Institute of Biomedical Engineering, National Chiao Tung University, Hsinchu, 30010, Taiwan, Republic of China.
E-mail address: wenurea@mail.nctu.edu.tw (W.L. Chen).
[1] These authors contribute equally to this work.

https://doi.org/10.1016/j.bios.2020.112111
Received 30 September 2019; Received in revised form 12 February 2020; Accepted 18 February 2020
Available online 20 February 2020

modification to increase biosensor stability (Dundas et al., 2013). Thus, biosensors produced in this way possess greater reproducibility, accuracy, and stability (three characteristics integral to POC products) than those produced with other methods, as shown by a human immunoglobulin A sensor designed by Minamiki et al., (2015). However, despite these innovations, POC guidelines demand specifically high levels of reproducibility, accuracy, and stability before biosensors can be considered for POC use.

According to the Clinical and Laboratory Standards Institute (CLSI; EP05-A3, EP24-A2, EP25-A), coefficient of variation (CV) less than 10% for reproducibility, accuracy, and stability are required. Therefore, further improvements to biosensors are necessary, specifically regarding the electrodes and mediator, the two components that determine the reproducibility, accuracy, and stability of all electrochemical biosensors. In terms of electrode assembly, SMT production settings can be adjusted to fit label-free affinity detection. This detection method measures changes in electrical signal directly on the surface of the chip, and accuracy is therefore highly dependent on electrode production settings. The thickness of the thin-film metal and surface topography (roughness) are two vital contributors to accuracy and can drastically affect conductivity and consistency, respectively (Butterworth et al., 2019), and ultimately affect the detection results. Consequently, calibration of the SMT production settings presents the opportunity to considerably improve accuracy. Meanwhile, despite the improvements in stability achieved using a streptavidin biomediator, immobilization of the bioreceptor directly onto the mediator limits its orientation and interferes with function, thus limiting accuracy (Trilling et al., 2013). Introducing a linker to the biomediator has been shown to be a feasible solution; however, the optimal linker sequence to maximize accuracy remains unclear and requires further research (Ikonomova et al., 2018).

The goal of this research was to develop a semiconductor manufacturing electrochemical biosensor (SMEB) platform that combines improved SMT production settings with a unique streptavidin biomediator to produce label-free affinity electrochemical biosensors suitable for POC use. The thickness and roughness of the electrodes were calibrated to optimize the reproducibility of label-free affinity detection, while a unique linker with ideal flexibility as well as rigidity was added to the streptavidin biomediator to improve accuracy. To prove functionality, a finished sensor was tested using protein samples to confirm reproducibility, accuracy, and stability. After verification of performance, different biosensors were constructed to detect other common POC targets, including circulating tumor cells (CTCs), DNA/RNA, and small compounds (e.g. curcumin), and their functionality was tested. Additionally, to optimize the platform for future development of a POC diagnosis kit, the guidelines for POC product development (Siontorou and Batzias 2010) were followed. This involved collaborating with manufacturers and making improvements, including modification of standard operating procedure (SOP) definitions, optimization of reaction conditions, simplification of measurement technology, and customization of the detection machine. Overall, the SMEB platform shows strong potential for integration in POC products for various purposes, such as food safety monitoring, environmental monitoring, disease diagnostics, and clinical guidance.

2. Materials and methods

2.1. Materials and apparatus

The pET-30a(+) vector was purchased from Novagen, Inc., and isopropyl β-D-1-thiogalactopyranoside (IPTG), mercaptoundecanoic acid (11-MUA), N-ethyl-N'-(3-dimethylaminopropyl) carbodiimide hydrochloride (EDC), N-hydroxysuccinimide (NHS), and curcumin powder were purchased from Sigma Aldrich, Inc. Ni-NTA resin was ordered from BioSmart, Inc. and an NHS-PEG$_4$-biotinylation kit was purchased from Thermo Fisher Scientific, Inc. Anti-cardiac troponin I (cTnI) antibody was ordered from Proteintech, Inc. cTnI native protein was ordered from Mybiosource, Inc. Anti-cytokeratin 7 (CK7) antibody was purchased from GeneTex, Inc. All aqueous solutions were prepared using ultrapure water from a Milli-Q Direct machine, and all oligonucleotides (DNA probe and DNA fragments) were synthesized by Tri-I Biotech, Inc.

The surface topography of the bio-chips was examined using a scanning electron microscope (SEM; Hitachi SU8010) at an accelerating voltage of 15 keV, and all electrochemical measurements were performed using a CH Instrument 920D (CHI 920D; CH instruments, Austin, TX, USA). Development of the final customized device was achieved through cooperation with Zensor R&D, Inc.

2.2. Electrode production

Gold thin-film electrodes were produced using direct plate copper (DPC) technology via a sputtering and etching process, illustrated in Fig. 1A, which is identical to SMT electrode production (Hierlemann et al., 2003). In this study, electrode settings were adjusted to a thickness greater than 0.1 μm and a surface roughness less than 0.3 μm. To evaluate the quality of production, the electrodes were examined using X-ray fluorescence spectroscopy and an alpha-step profiler; the results are shown in Fig. 1B.

2.3. Biomediator production

For the biomediator, two types of linker, GS linker (G_4S_1) and GW linker (GINSSSVPGDPPW) (Lower et al., 2005), were independently constructed with the streptavidin sequence and were cloned into the pET-30a(+) vector for recombinant protein expression. *Escherichia coli* (*E. coli*) DH5α was selected as the host for plasmid cloning and propagation (Fig. S1A), while *E. coli* BL21 (DE3) was used as the host for recombinant protein expression. Protein expression was regulated by IPTG induction and protein purification was executed through a standard Ni-NTA column protocol (Fig. S1B).

2.4. SMEB platform fabrication

Establishment of the SMEB platform consisted of five steps from self-assembled monolayer (SAM) formation to bioreceptor modification (Fig. 2A). First, SAMs were established on the gold surface by immersing the electrodes in an ethanolic solution of 11-MUA (Stettner et al., 2009). The carboxyl-terminated group of 11-MUA was then activated through the EDC and NHS coupling reaction (Palazon et al., 2014; Tsai et al., 2019). The electrodes were rinsed and immersed in the biomediator protein solution (conc. 10 μg/mL). After the biomediator was immobilized on the gold surface by covalent bonding, the electrodes were washed and blocked with 3% gelatin solution. To immobilize the bioreceptors (antibody, DNA probe and functional protein) on the electrodes, NHS-PEG$_4$-biotinylation was performed and biotinylated bioreceptors were added to the surface of the biomediator-modified electrodes. Finally, the electrodes were washed and dried, and electrochemical impedance spectroscopy (EIS) was performed to verify the entire process of SMEB platform fabrication (Fig. 2B). Electrodes were stored at 4 °C for subsequent use.

2.5. Electrochemical measurements

For EIS measurements, a frequency range of 0.1–1 kHz with an amplitude of 10 mV was set to execute scanning, ZSimpWin was used to analyze the EIS data, and Randles' equivalent circuit R(Q(RW)) was applied to simulate the value of the charge transfer resistance (Rct) as a sample detection value. For differential pulse voltammetry (DPV) measurements, a potential range of 0.6 V to -0.6 V and amplitude of 50 mV were selected to perform scanning and the sample detection value was acquired from the absolute value of the maximum detected current. All EIS and DPV values were normalized by subtracting the blank values obtained from measuring the solution without target analytes. Based on

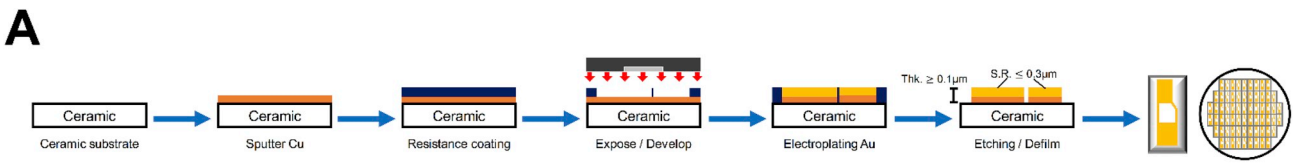

B

a. Thin film thickness of measurement

Instrument: X-ray fluorescence spectroscopy

Spec.	USL	LSL	No. 1	No. 2	No. 3	Max.	Min.	Avg.	Std.	Judgement
Thk. ≥ 0.1 μm	---	0.10	0.122	0.124	0.116	0.124	0.116	0.121	0.0034	PASS

b. Surface roughness test

Instrument: Alpha-Step® D-500 Stylus Profiler

Spec.	USL	LSL	No. 1	No. 2	No. 3	Max.	Min.	Avg.	Std.	Judgement
S.R. ≤ 0.3 μm	0.30	0.00	0.070	0.100	0.090	0.100	0.070	0.087	0.0124	PASS

Fig. 1. Production of electrodes. (A) Schematic illustration of electrode fabrication. (B) Production setting confirmation using X-ray fluorescence spectroscopy for thickness (μm) determination and an Alpha-Step® D-500 Stylus Profiler for surface roughness (μm) evaluation. Spec.: specification; USL: upper specification limit; LSL: lower specification limit; No.: chip number; Max.: maximum; Min.: minimum; Avg.: average; Std.: standard deviation.

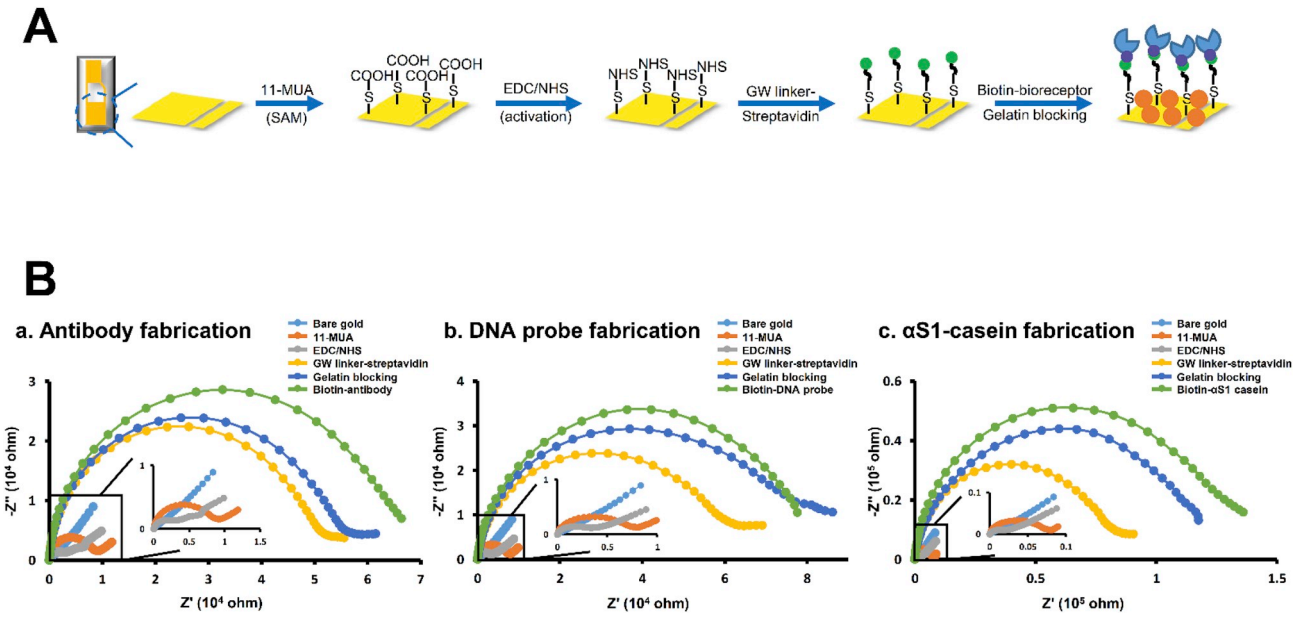

Fig. 2. SMEB platform fabrication. (A) Schematic illustration of SMEB platform fabrication. (B) EIS measurements to verify the steps of antibody (a), DNA probe (b) and αS1-casein (c) platform fabrication.

the obtained results (Fig. S2), EIS was selected for protein and CTC detection, and DPV was selected for detection of DNA/RNA and small compounds.

2.6. Calculation of reproducibility, accuracy, and stability

Reproducibility was calculated based on the coefficient of variation (CV; equation (1)) value of the Rct values measured from each chip after production to represent the consistency of production and signal detection.

$$\textbf{Coefficient of variation (CV)} = \frac{\textit{Standard deviation (SD)}}{\textit{average of detection value } (\bar{S})} \times 100\% \quad (1)$$

Accuracy describes the variation between biosensor-detected values and the actual values. In tests of unknown samples shown in Fig. 4, realistic values were determined by the gold standard method in the hospital. The accuracy values of SMEB detection results were calculated by equation (2) and are shown in Table 1.

$$\textbf{Accuracy} = 100\% - |\textbf{Relative deviation (RD)}| = 100\% - \left|\frac{\textit{Detection value} - \textit{Realistic value}}{\textit{Realistic value}} \times 100\%\right| \quad (2)$$

Stability describes the variation in detection signals during a period of long-term storage. As shown in Fig. 5, the baseline of each analyte concentration was determined by the average of the values detected every week and RD of the detection values compared to the baseline was calculated to deduce the stability value by equation (3).

$$\textbf{Stability} = 100\% - |\textbf{Relative deviation (RD)}| = 100\% - \left|\frac{\textit{Week detection value } (W) - \textit{baseline } (\overline{W})}{\textit{baseline } (\overline{W})} \times 100\%\right| \quad (3)$$

3. Results

To improve biosensor performance and fulfill the POC guidelines set by the CLSI, SMT production settings were calibrated to produce electrodes with a thickness greater than 0.1 μm and a surface roughness less than 0.3 μm to complement label-free affinity detection (Fig. 1). A GW linker was also fused to the streptavidin biomediator to optimize flexibility and rigidity (Fig. 2), and thereby improve function. Functionality was evaluated using cardiac troponin I (cTnI) to confirm that reproducibility, accuracy, and stability all had CV of less than 10%.

3.1. Production consistency and detection reproducibility

Robust electrode consistency is essential to improve biosensor reproducibility. EIS was therefore performed on five chips produced from the same batch after electrode assembly and the CV was calculated to assess consistency. The calibrated settings improved the CV from 15.92% for the chips produced with original settings to 3.03% (Fig. 3A and SEM images), and thus improved consistency. Next, the effects of the calibrated settings, as well as the improved biomediator (with GW linker), on modified chip consistency were investigated by performing EIS on four different sets of five modified chips, as shown in Fig. 3B and the respective SEM images. In chips produced with the original SMT production settings, changing the original biomediator (Fig. 3Ba) to the improved biomediator (Fig. 3Bb) lowered the CV from 21.43% to 9.2%, indicating that modifying the five chips with the improved biomediator significantly improved consistency. Likewise, in chips with the original biomediator, using the calibrated settings (Fig. 3Bc) instead of the original settings (Fig. 3Ba) improved the CV from 21.43% to 7.22%, again demonstrating improved consistency. Combining the calibrated settings and modified biomediator resulted in the most substantial improvement to consistency between chips, lowering the CV to 1.65%, as shown in Fig. 3Bd. In addition, consistency between production batches was confirmed (Fig. 3C). EIS of three different batches of modified chips with improved components yielded a CV of 1.82%, suggesting that calibration of the production settings and the improved biomaterials considerably elevated consistency. The functionality and reproducibility of the final product were then evaluated by using a fully constructed biosensor to detect cTnI (Fig. 3D). Fig. 3Da indicates that increased antigen concentrations elicited stronger impedance signals, thereby verifying functionality. Biosensors were then constructed using chips from different batches to demonstrate post-modification consistency across the production process. High reproducibility was achieved, regardless of batch origination (Fig. 3Db). Overall, the combination of optimized SMT production settings and the improved biomediator greatly enhanced the consistency of the modified chips, resulting in significantly improved detection reproducibility.

3.2. Accuracy and stability

To determine the accuracy of the improved biosensor, cTnI detection in whole blood was assessed. Whole blood samples were collected and analyzed using both the improved biosensor in the laboratory and the gold standard method in the hospital. Similar results were observed between the SMEB platform and the hospital method (Fig. 4). In addition, the SMEB results showed low relative deviation from the hospital results; specifically, relative deviation was limited to 7% across all samples (Table 1), indicating a minimum accuracy of 93%. Overall, these results suggest that biosensors produced with the SMEB platform show strong potential to maintain accuracy and high clinical feasibility once integrated into POC applications.

Table 1
cTnI detection in whole blood samples.

Sample no.	SMEB (ng/mL)	Hospital (ng/mL)	Accuracy (%)
1	**0.00**	**N.D.**	**-**
2	**0.00**	**N.D.**	**-**
3	**0.02**	**N.D.**	**-**
4	**0.00**	**N.D.**	**-**
5	**1.74**	**1.64**	**93.91**
6	**4.28**	**4.02**	**93.54**
7	**0.35**	**0.37**	**94.60**
8	**0.72**	**0.71**	**98.60**
9	**0.20**	**0.19**	**94.74**
10	**0.62**	**0.64**	**96.88**
11	**3.19**	**3.08**	**96.43**

After confirming the consistency of reproduction across all stages of the SMEB platform (Fig. 3A-C), storage stability was examined by storing a batch of the electrodes at room temperature (RT) in a drier and investigating their function over a period of nine weeks. Consistent maintenance of the signal was achieved over time (Fig. 5); the signal variation over nine weeks was limited to 6%. This suggests stability of the SMEB platform is 94%, which is appropriate for POC use.

3.3. Applications

To demonstrate the capabilities of the completed SMEB platform, three different biosensors were constructed (Fig. 2B) to detect circulating tumor cells (CTCs), DNA/RNA, and curcumin (Fig. S3).

3.3.1. CTC detection

CTCs are important indicators of progression in various cancers. To simulate detection of CTCs in patients with cancer, blood samples were obtained from a healthy individual and a patient with lung cancer from Shuang Ho Hospital. Flow cytometry performed at the hospital indicated the presence of cytokeratin 7 (CK7), a biomarker associated with lung cancer CTCs, in the blood sample of the lung cancer patient. CK7 was therefore chosen as the detection target, and a biosensor was constructed using an anti-CK7 antibody-modified chip for detection. The detection results (Fig. 6Ab) deduced from the calibration curve demonstrated a detection sensitivity of 2 target cells in 1 mL solution (Fig. 6Aa), indicating functional CTC biomarker detection.

3.3.2. DNA/RNA detection

DNA/RNA concentrations are often examined to monitor changes in gene expression in cells. For example, YKL 40 is an inflammatory factor in many cancers and may indicate changes in gene expression or even cancer cell transition/migration (Jefri et al., 2015). Therefore, to mimic realistic POC settings, anti-YKL-40 DNA probe-modified chips were used to detect YKL-40 fragments in total RNA of different lung cancer cell lines. The detection results (Fig. 6Bb) deduced from the calibration curve revealed a limit of detection (LOD) of 1 fM (Fig. 6Ba). High readings were detected in H1975 cells, and low readings were detected in H292 and HCC827 cells, consistent with the results of PCR.

3.3.3. Curcumin detection

Assessment of the concentrations of functional compound is critical to some types of agriculture. For example, curcumin is important in turmeric cultivation. Therefore, detection of curcumin dissolved in ethanol was performed using αS1-casein-modified chips (αS1-casein has a high binding affinity for curcumin (Sneharani et al., 2009)). The detection results (Fig. 6Cb) deduced from the calibration curve suggested the LOD was 10 pM (Fig. 6Ca), indicating functional curcumin detection. These results were consistent with those obtained using high-performance liquid chromatography (HPLC).

3.4. Preparation for POC use

First, a SOP was defined to optimize SAM formation and bioreceptor modification for highly accurate and consistent detection signals in each production batch. The reaction time was then investigated; when the antigen concentration was greater than 100 pg/mL, only 10 min of reaction time were required for accurate detection (Fig. 7A). Next, to simplify measurement, the sensitivity of various measurement frequencies was tested. A frequency of 0.1 Hz yielded the highest sensitivity (Fig. 7B) and was deemed optimal. Finally, detection using a biosensor produced with the SMEB platform was demonstrated in a video recording.

Supplementary video related to this article can be found at https://doi.org/10.1016/j.bios.2020.112111.

4. Discussion

Numerous factors can seriously affect the reproducibility, accuracy, and stability of biosensors, and have resulted in much attention in the fields of sensing towards optimizing biosensors. Most recent platforms achieved improved reproducibility, accuracy, or stability individually by adjusting either the electrodes or surface materials via different methods of biosensor production. These developments include enhanced accuracy through integration of highly vertical ZnO nanorods (Shrivastava et al., 2017), incorporation of covalent organic framework (COF) materials into sensing fields (Liu et al., 2019), use of fluorescence (Lee et al., 2017), and application of electrochemical immunodetection (Yang et al., 2019), as well as superior reproducibility through use of a platinum network as a counter electrode (Zhao et al., 2018), utilization of sulfur−nitrogen co-doped ordered mesoporous carbon (SN-OMC) and thymine−Hg2+−thymine (T−Hg2+−T) mismatch structure as

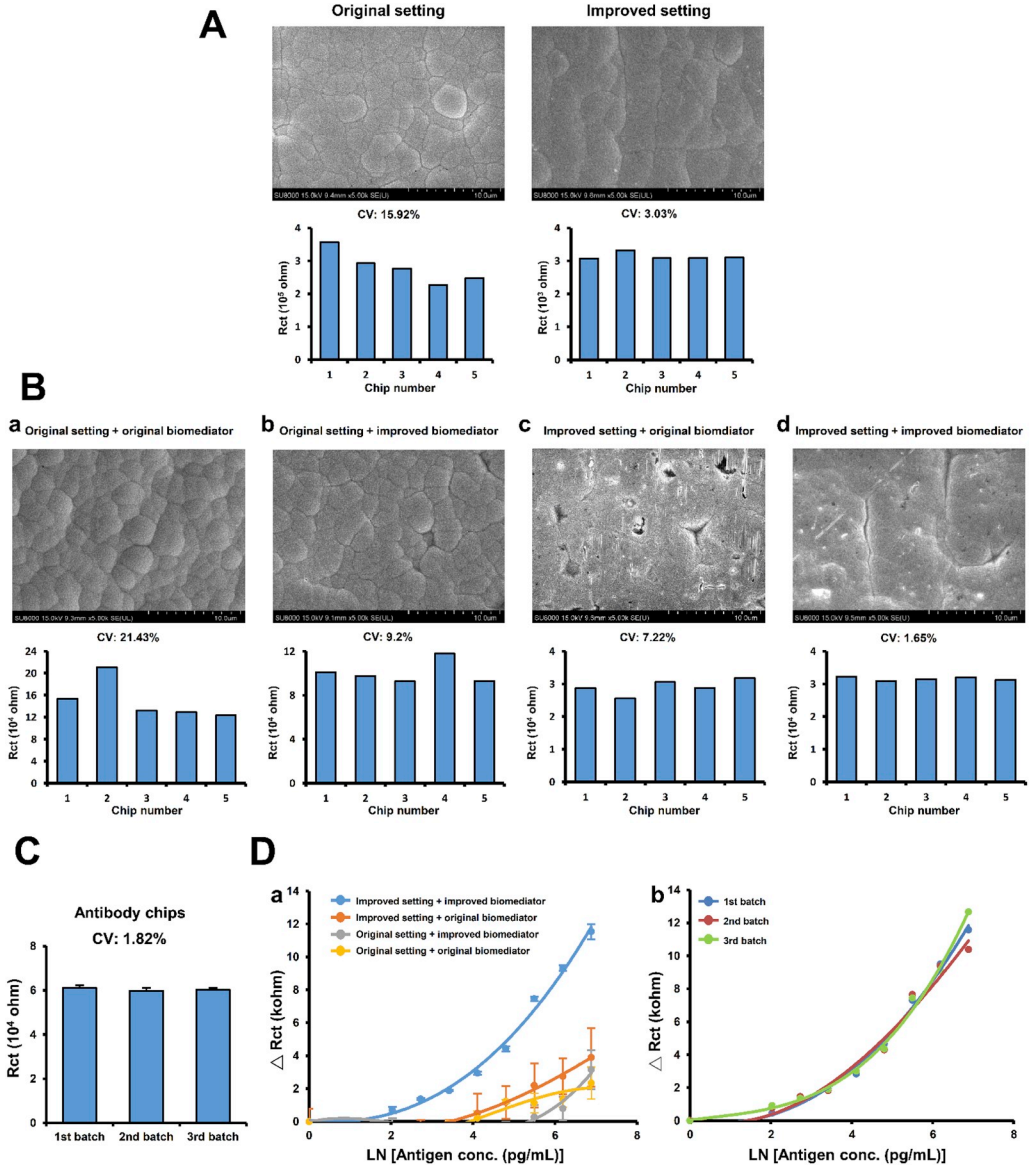

Fig. 3. Reproducible SMEB platform establishment. (A) Consistency analysis using SEM and EIS of bare chips produced with original and improved settings. (B) SEM and EIS consistency analysis of modified chips produced with original settings + original biomediator (a), original settings + improved biomediator (b), improved settings + original biomediator (c), and improved settings + improved biomediator (d). (C) EIS consistency analysis of different batches produced with the improved settings + improved biomediator-modified chips. (D) Functional verification of anti-cTnI antibody-modified chips and cTnI antigen based on measuring EIS in different settings + biomediator combinations (a) and in different batches (b).

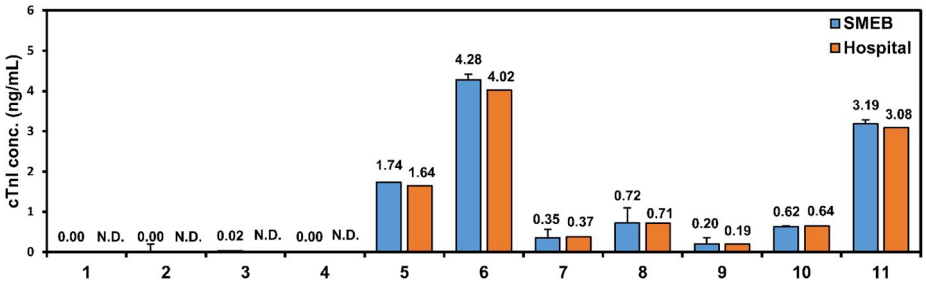

Fig. 4. Examination of the accuracy of the SMEB platform using anti-cTnI antibody-modified chips to detect cTnI antigen in whole blood samples. The actual concentrations were verified using the gold standard method in the hospital. (For interpretation of the references to colour in this figure legend, the reader is referred to the Web version of this article.)

electrochemical aptasensors (Lai et al., 2018), and development of imprinted molecular sensors (Fu et al., 2019). However, POC guidelines demand high performance in all three aspects (reproducibility, accuracy, and stability).

This research focused on resolving the limiting drawbacks of two highly advantageous production techniques—SMT-produced electrodes and streptavidin biomediators—to provide excellent reproducibility, accuracy, and stability at the same time. The combination of SMT production settings optimized for label-free affinity detection (Fig. 1) and a biomediator produced with a linker of ideal flexibility and rigidity (Fig. 2A) was investigated as a method of developing an electrochemical biosensor that possesses reproducibility, accuracy, and stability suitable for POC use. Calibrating electrode thickness to greater than 0.1 μm and surface roughness to less than 0.3 μm allowed our chips to perform better label-free affinity detection, and also improved the consistency of electrode assembly (Fig. 3). Previous studies demonstrated that current production settings do not fall in these ranges and have lower detecting consistency (Butterworth et al., 2019; Hierlemann et al., 2003). Inclusion of a GW linker with both flexibility and rigidity (Lower et al., 2005) to improve the biomediator ensures that the bioreceptor is properly immobilized and that its function is not hindered by limited orientation (Caroselli et al., 2018; Trilling et al., 2013), while maintaining enough distance between the receptor domain and chip to preserve function (Chen et al., 2013; Li et al., 2016).

To validate these improvements, several experiments involving detection of cTnI were conducted to assess various aspects of performance. First, reproducibility was investigated. Fig. 3A and Fig. 3Bc show the improved consistency from calibrated settings in bare and modified chips, respectively. Fig. 3Bb shows the increased consistency achieved through uniform immobilization of the bioreceptor facilitated by the improved biomediator. Comparison between the SEM images in Fig. 3A as well as between those in Fig. 3B show no visible differences in commonly modified parameters, such as gap etching size, suggesting that the decreased CV in the modified chips resulted directly from optimized calibration of the settings and unique biomediator, respectively. Fig. 3Bd shows the consistency of chips modified with both improvements, while Fig. 3C and Fig. 3D show high consistency between batches and high detection reproducibility, respectively. While the modifications improved chip consistency individually, the combination of both optimized settings and unique biomediator was essential to achieving reproducibility that meets POC guidelines.

Accuracy was investigated next (Fig. 4), with the comparison between detection by the proposed biosensor and hospital tests revealing low relative deviation and high alignment with the gold standard method performed by the hospital, and thus high accuracy. This is likely due to the modified electrode thickness and surface roughness increasing conductivity (Butterworth et al., 2019; Hierlemann et al., 2003) and generally complementing label-free affinity detection. Finally, the stability of the proposed biosensor was evaluated by assessing signal maintenance over a period of nine weeks. Fig. 5 shows variation over this period was limited to 6%, suggesting stability suitable for POC use.

Optimization of SMT production settings, combined with a unique biomediator, allowed the development of a biosensor with greater reproducibility, accuracy, and stability than current products achieve. Importantly, the CVs of all three of these qualities were improved to less than 10%, in accordance with the guidelines determined by the CLSI (EP05-A3, EP24-A2, EP25-A). Using this platform, various biosensors were constructed to assess their ability to detect common POC targets including CTCs, DNA/RNA, and curcumin (Fig. 6). In terms of CTC detection, the biosensors demonstrated a detection limit of 2 cells/mL (Fig. 6A), which is far superior to the detection limit of 52.24 cells/mL in a recent study (Chen et al., 2019). For nucleic acid detection, this study achieved a LOD of 1 fM (Fig. 6B), which is more sensitive than recently reported detection at picomolar level (Aoki et al., 2019). Lastly, our biosensors showed a LOD of 10 pM for curcumin (Fig. 6C), while a

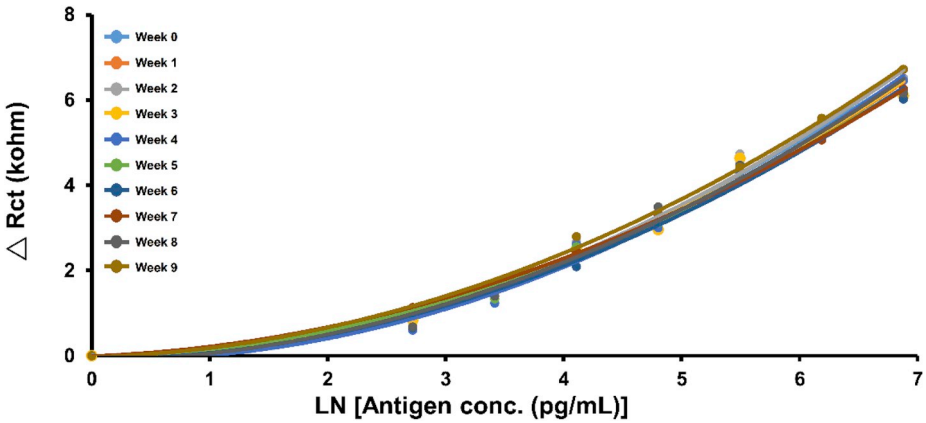

Fig. 5. Stability analysis of the SMEB platform during storage at RT for nine weeks, using anti-cTnI antibody-modified chips to detect cTnI antigen by EIS every week.

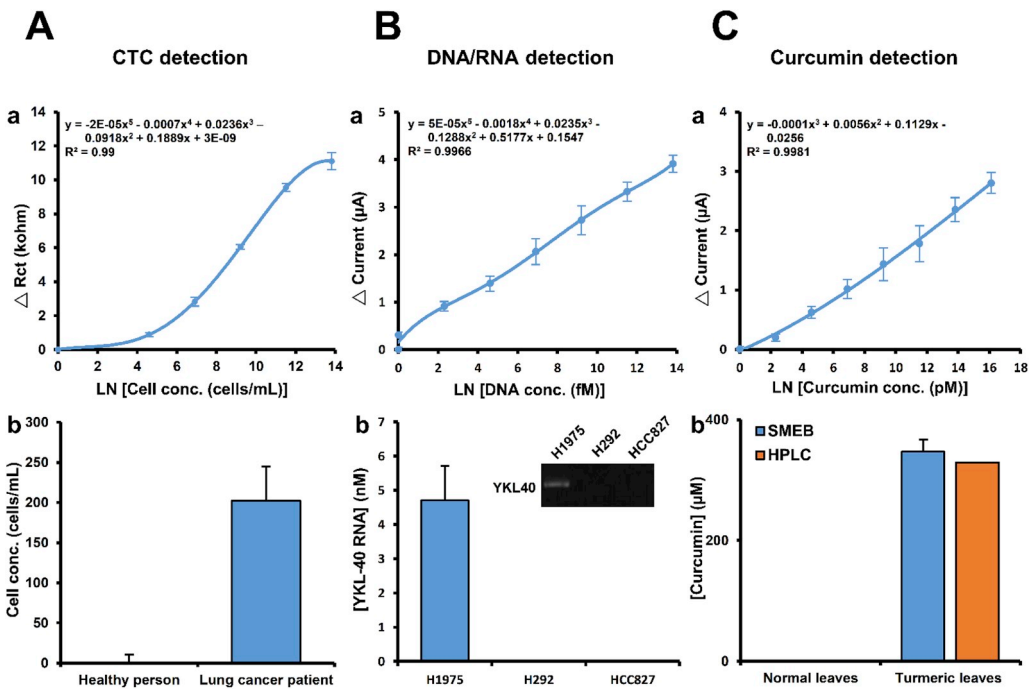

Fig. 6. SMEB platform applications. (A) Detection of circulating tumor cells (CTCs) using anti-CK7 antibody-modified chips and EIS. Calibration curve (a) and results for whole blood samples from a healthy individual and a patient with lung cancer (b). (B) DNA/RNA detection using anti-YKL-40 DNA probe (5'-TTAGGGTGGTAAAATGCTGTT-3')-modified chips, YKL-40 DNA fragment (5'-AACAGCATTTTACCACCCTAA-3'), and measurement by DPV. Calibration curve (a) and total RNA (H1975, H292 and HCC827 cell lines) detection (b); the results were consistent with PCR analysis (b). (C) Curcumin detection using αS1-casein-modified chips and DPV. Calibration curve (a) and curcumin detection from normal leaves and turmeric leaves (b); the results were consistent with HPLC analysis (b).

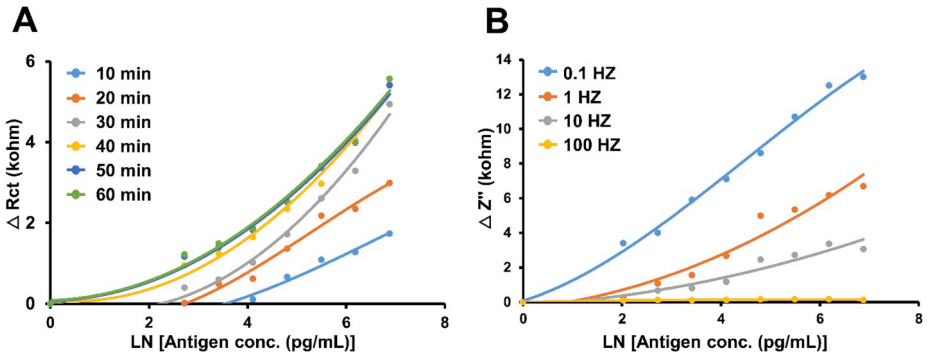

Fig. 7. Optimization for POC use. (A) Reaction time investigation using anti-cTnI antibody-modified chips to detect cTnI antigen after different antigen reaction times (from 10 min to 60 min). (B) Measurement simplification from broad frequency scanning (EIS) to fixed frequency scanning (IMPT). The tested frequencies included 0.1, 1, 10 and 100 Hz at an amplitude of 10 mV.

previous study indicated a curcumin detection limit of 0.109 μM in human blood serum (Zokhtareh and Rahimnejad 2018). The proposed biosensors made with improved electrodes and biomediator were able to break through the current limits of detection for CTCs, DNA/RNA, and curcumin and may prove useful in the development of various products designed to detect common POC targets. Finally, to prepare the platform for POC use, we investigated reaction time (Fig. 7A), simplified the reaction measurement (Fig. 7B), miniaturized the device, and recorded a demonstration video to ensure quick detection, portability, and ease of use, three key characteristics of POC products (Baryeh et al., 2017). Through this research, we have developed a platform capable of producing biosensors that possess exceptional reproducibility, accuracy, and stability, and show exceptional promise for successful integration in POC applications.

5. Conclusion

This project aimed to establish a platform capable of producing biosensors with reproducibility, accuracy, and stability that meet the POC guidelines set by the CLSI. The settings for SMT production of the electrodes were optimized, calibrating thickness to greater than 0.1 μm and surface roughness to less than 0.3 μm. In addition, the streptavidin biomediator was improved through addition of a GW linker, which provides both ideal flexibility and rigidity for bioreceptor immobilization and thus performs better than previously used linkers. These improvements considerably enhanced performance, allowing all three required characteristics (reproducibility, accuracy, and stability) to meet POC standards. To demonstrate the wide range of the platform, biosensors were produced to prove functionality for detection of CTCs, DNA/RNA, and small compounds, three common types of POC targets. Finally, steps were taken to optimize the platform for future use in realistic applications, by defining a SOP for mass production and ensuring storage stability. In summary, this SMEB platform simultaneously achieves reproducibility, accuracy, and stability and is suitable for integration into a wide variety of POC products.

Declaration of competing interest

The authors declare that they have no known competing financial interests or personal relationships that could have appeared to influence the work reported in this paper.

CRediT authorship contribution statement

Lung-Chieh Chen: Conceptualization, Methodology, Investigation, Writing - original draft, Visualization. **Erick Wang:** Writing - original draft, Writing - review & editing. **Chun-San Tai:** Investigation, Writing - review & editing, Visualization. **Yuan-Chen Chiu:** Investigation, Visualization. **Chang-Wei Li:** Resources. **Yan-Ren Lin:** Resources. **Tsung-Han Lee:** Resources. **Ching-Wen Huang:** Resources. **Jung-Chih Chen:** Resources, Methodology. **Wen Liang Chen:** Conceptualization, Methodology, Visualization, Writing - review & editing, Supervision.

Acknowledgements

This work was supported in part by the Green and Intelligent Agricultural System and the Spatiotemporal Control of Epithelial to Mesenchymal Transition by Tantalum Oxide Artificial Microenvironments: The Next Step towards Personalized Medicine sponsored by Taiwan Ministry of Science and Technology [grant numbers MOST 106-2314-B-009-001, 106-3114-8-009-004, and 107-2823-8-009-004]; and in part by the Novel Bioengineering and Technological Approaches to Solve Two Major Health Problems in Taiwan sponsored by the Taiwan Ministry of Science and Technology Academic Excellence Program [grant number MOST 108-2633-B-009-001].

Appendix A. Supplementary data

Supplementary data to this article can be found online at https://doi.org/10.1016/j.bios.2020.112111.

Funding

<Ministry of Science and Technology>
Grant Number: MOST 106-2314-B-009-001, 106-3114-8-009-004, 107-2823-8-009-004, 108-2633-B-009-001.gs5

References

Anik, Ü., 2017. Electrochemical medical biosensors for POC applications. Medical Biosensors for Point of Care (POC) Applications 275–292.
Aoki, H., Corn, R.M., Matthews, B., 2019. MicroRNA detection on microsensor arrays by SPR imaging measurements with enzymatic signal enhancement. Biosens. Bioelectron. 142, 111565.
Baryeh, K., Takalkar, S., Lund, M., Liu, G., 2017. Introduction to medical biosensors for point of care applications. Medical Biosensors for Point of Care (POC) Applications 3–25.
Butterworth, A., Blues, E., Williamson, P., Cardona, M., Gray, L., Corrigan, D.K., 2019. SAM composition and electrode roughness affect performance of a DNA biosensor for antibiotic resistance. Biosensors (Basel) 9 (1).
Caroselli, R., Garcia Castello, J., Escorihuela, J., Banuls, M.J., Maquieira, A., Garcia-Ruperez, J., 2018. Experimental study of the oriented immobilization of antibodies on photonic sensing structures by using protein A as an intermediate layer. Sensors (Basel) 18 (4).
Chen, X., Zaro, J.L., Shen, W.C., 2013. Fusion protein linkers: property, design and functionality. Adv. Drug Deliv. Rev. 65 (10), 1357–1369.
Chen, Y., Peng, J., Lai, Y., Wu, B., Sun, L., Weng, J., 2019. Ultrasensitive label-free detection of circulating tumor cells using conductivity matching of two-dimensional semiconductor with cancer cell. Biosens. Bioelectron. 142, 111520.
da Silva, E.T.S.G., Souto, D.E.P., Barragan, J.T.C., Giarola, J.de F., deMoraes, A.C.M., Kubota, L.T., 2017. Electrochemical biosensors in point-of-care devices: recent advances and future trends. ChemElectroChem 4 (4), 778–794.
Daniels, J.S., Pourmand, N., 2007. Label-free impedance biosensors: opportunities and challenges. Electroanalysis 19 (12), 1239–1257.
Dundas, C.M., Demonte, D., Park, S., 2013. Streptavidin-biotin technology: improvements and innovations in chemical and biological applications. Appl. Microbiol. Biotechnol. 97 (21), 9343–9353.
Fu, K., Zhang, R., He, J., Bai, H., Zhang, G., 2019. Sensitive detection of ketamine with an electrochemical sensor based on UV-induced polymerized molecularly imprinted membranes at graphene and MOFs modified electrode. Biosens. Bioelectron. 143, 111636.
Hierlemann, A., Brand, O., Hagleitner, C., Baltes, H., 2003. Microfabrication techniques for chemical/biosensors. Proc. IEEE 91 (6), 839–863.
Ikonomova, S.P., Le, M.T., Kalla, N., Karlsson, A.J., 2018. Effect of linkers on immobilization of scFvs with biotin-streptavidin interaction. Biotechnol. Appl. Biochem. 65 (4), 580–585.
Jefri, M., Huang, Y.N., Huang, W.C., Tai, C.S., Chen, W.L., 2015. YKL-40 regulated epithelial-mesenchymal transition and migration/invasion enhancement in non-small cell lung cancer. BMC Canc. 15, 590.
Johnson, S., Krauss, T.F., 2017. Label-free affinity biosensor arrays: novel technology for molecular diagnostics. Expet Rev. Med. Dev. 14 (3), 177–179.
Lai, C., Liu, S., Zhang, C., Zeng, G., Huang, D., Qin, L., Liu, X., Yi, H., Wang, R., Huang, F., Li, B., Hu, T., 2018. Electrochemical aptasensor based on sulfur-nitrogen codoped ordered mesoporous carbon and thymine-Hg(2+)-thymine mismatch structure for Hg(2+) detection. ACS Sens. 3 (12), 2566–2573.
Lee, W.I., Shrivastava, S., Duy, L.T., Yeong Kim, B., Son, Y.M., Lee, N.E., 2017. A smartphone imaging-based label-free and dual-wavelength fluorescent biosensor with high sensitivity and accuracy. Biosens. Bioelectron. 94, 643–650.
Li, G., Huang, Z., Zhang, C., Dong, B.J., Guo, R.H., Yue, H.W., Yan, L.T., Xing, X.H., 2016. Construction of a linker library with widely controllable flexibility for fusion protein design. Appl. Microbiol. Biotechnol. 100 (1), 215–225.
Liu, X., Huang, D., Lai, C., Zeng, G., Qin, L., Wang, H., Yi, H., Li, B., Liu, S., Zhang, M., Deng, R., Fu, Y., Li, L., Xue, W., Chen, S., 2019. Recent advances in covalent organic frameworks (COFs) as a smart sensing material. Chem. Soc. Rev. 48 (20), 5266–5302.
Lower, B.H., Yongsunthon, R., Vellano 3rd, F.P., Lower, S.K., 2005. Simultaneous force and fluorescence measurements of a protein that forms a bond between a living bacterium and a solid surface. J. Bacteriol. 187 (6), 2127–2137.
Minamiki, T.M., T, Sasaki, Y., Kurita, R., Niwa, O., Wakida, S., Tokito, S., 2015. An organic field-effect transistor with an extended-gate electrode capable of detecting human immunoglobulin A. Anal. Sci. 31, 725–728.
Palazon, F., Benavides, C.M., Leonard, D., Souteyrand, E., Chevolot, Y., Cloarec, J.P., 2014. Carbodiimide/NHS derivatization of COOH-terminated SAMs: activation or byproduct formation? Langmuir 30 (16), 4545–4550.
Pohanka, M., 2017. Biosensors based on semiconductors, a review. International Journal of Electrochemical Science 6611–6621.
Shrivastava, S., Triet, N.M., Son, Y.M., Lee, W.I., Lee, N.E., 2017. Seesawed fluorescence nano-aptasensor based on highly vertical ZnO nanorods and three-dimensional quantitative fluorescence imaging for enhanced detection accuracy of ATP. Biosens. Bioelectron. 90, 450–458.
Siontorou, C.G., Batzias, F.A., 2010. Innovation in biotechnology: moving from academic research to product development–the case of biosensors. Crit. Rev. Biotechnol. 30 (2), 79–98.
Sneharani, A.H., Singh, S.A., Appu Rao, A.G., 2009. Interaction of alphaS1-casein with curcumin and its biological implications. J. Agric. Food Chem. 57 (21), 10386–10391.
Stettner, J., Frank, P., Griesser, T., Trimmel, G., Schennach, R., Gilli, E., Winkler, A., 2009. A study on the formation and thermal stability of 11-MUA SAMs on Au(111)/mica and on polycrystalline gold foils. Langmuir 25, 1427–1433.
Szunerits, S., Mishyn, V., Grabowska, I., Boukherroub, R., 2019. Electrochemical cardiovascular platforms: current state of the art and beyond. Biosens. Bioelectron. 131, 287–298.
Trilling, A.K., Beekwilder, J., Zuilhof, H., 2013. Antibody orientation on biosensor surfaces: a minireview. Analyst 138 (6), 1619–1627.
Tsai, T.C., Liu, C.W., Wu, Y.C., Ondevilla, N.A.P., Osawa, M., Chang, H.C., 2019. In situ study of EDC/NHS immobilization on gold surface based on attenuated total reflection surface-enhanced infrared absorption spectroscopy (ATR-SEIRAS). Colloids Surf. B Biointerfaces 175, 300–305.
Yang, T., Ren, X., Yang, M., Li, X., He, K., Rao, A., Wan, Y., Yang, H., Wang, S., Luo, Z., 2019. A highly sensitive label-free electrochemical immunosensor based on poly (indole-5-carboxylicacid) with ultra-high redox stability. Biosens. Bioelectron. 141, 111406.
Zhao, L., Han, H., Ma, Z., 2018. Improved screen-printed carbon electrode for multiplexed label-free amperometric immuniosensor: addressing its conductivity and reproducibility challenges. Biosens. Bioelectron. 101, 304–310.
Zokhtareh, R., Rahimnejad, M., 2018. A novel sensitive electrochemical sensor based on nickel chloride solution modified glassy carbon electrode for curcumin determination. Electroanalysis 30 (5), 921–927.